PNAS
www.pnas.org

Supplementary Information for

Prosurvival kinase PIM2 is a therapeutic target for eradication of chronic myeloid leukemia stem cells

Leyuan Ma, Magnolia L. Pak, Jianhong Ou, Jun Yu, Pamela St. Louis, Yi Shan, Lloyd Hutchinson, Shaoguang Li, Michael A. Brehm, Lihua Julie Zhu, and Michael R. Green

Corresponding author: Michael R. Green
Email: Michael.Green@umassmed.edu

This PDF file includes:

Supplementary Materials and Methods
Figs. S1 to S11
Tables S1 to S2
Caption for Dataset S1
References for SI reference citations

Other supplementary materials for this manuscript include the following:

Dataset S1

www.pnas.org/cgi/doi/10.1073/pnas.1903550116

Supplementary Materials and Methods

Single Cell Sorting and cDNA Synthesis. Samples CML1-3 (Table S1) were enriched for CD34+ cells using magnetic beads (Miltenyi Biotech). CD34+ cells were then stained with Pacific Blue-conjugated CD34 (cat. no. 48-0349, clone 4H11), APC-conjugated CD38 (cat. no. 17-0389, clone HIT2), PE-conjugated CD90 (cat. no. 12-0909, clone 5E10), and FITC-conjugated CD45RA (cat. no. 11-0458, clone HI100) antibodies, and 7-AAD (all from eBioscience). The CD34+CD38-CD90+CD45RA- population was then sorted using a BD FACSAria II flow cytometer (BD Biosciences) with FACSDIVA software at single-cell mode into 96-well plates containing lysis buffer (4 µl of 0.2% TritonX-100, 2 U/µl RNase in nuclease-free water). Plates were immediately spun at 800 g for 1 min and put on dry ice. Single cell lysates were processed immediately for cDNA synthesis according to a revised Smart-seq2 protocol (1, 2). Samples were processed immediately after collection or within two weeks to avoid severe degradation.

To identify wells that had successfully captured single cells, cDNAs were analyzed by qPCR for expression of two housekeeping genes, *B2M* and *GAPDH* (see Table S2 for primer sequences). The quality of cDNA was also evaluated using an Agilent 2100 Bioanalyzer. Only cDNAs showing expression of housekeeping genes and the expected fragment distribution (peaking at ~2 kb, with minimal noisy peaks below 500 bp; see Fig. S1*B*) were used for subsequent experiments. The typical concentration of cDNA obtained ranged from 0.1–11 ng/µl in a volume of 20 µl.

Nested qPCR to Identify BCR-ABL Transcripts in Single Cells. Two-step nested qPCR was performed as follows using primers listed in Table S2. The first round of PCR (10 µl total volume, 1 µl of undiluted single-cell cDNA as template) consisted of 1 cycle of 95°C for 3 min; 25 cycles of 95°C for 30 sec, 58°C for 30 sec, and 68°C for 30 sec; extension at 68°C for 5 min; and 4°C hold. The second round of qPCR (10 µl total volume, 1 µl of 10x diluted first-round PCR product as template) consisted of 1 cycle of 95°C for 3 min; 40 cycles of 95°C for 3 sec and 60°C for 30 sec. Nested qPCR reactions on single cells were carried out in technical quadruplicate, and only cells that were either positive or negative for BCR-ABL in all four replicates were selected for further analysis by RNA-seq.

To determine the false-positive and false-negative rates of the nested qPCR assay, two experiments were performed. First, 48 HSCs (CD34+CD38-CD90+CD45RA-) were sorted from cord blood, cDNA was isolated, and nested qPCR was performed for BCR-ABL. As a positive control, cDNA from 16 CMLSCs (CD34+CD38-CD90+CD45RA-) that had been previously identified as BCR-ABL+ cells by nested qPCR was used. The number of HSCs that showed positive amplification was determined (Fig. S1*D*, left). In a second experiment, single cells from the BCR-ABL- human lymphoblast U937 and BCR-ABL+ human CML KYO-1 cell lines were sorted, and cell lysate was isolated from single cells and split into two portions, half of which was used to carry out BCR-ABL gene-specific qRT-PCR (using the BCR-ABL-specific RT primer and BCR-ABL second-round nested qPCR primers; see Table S2 for sequences), and the other half of which was used for nested qPCR. It was first confirmed that each assay was sensitive enough to detect BCR-ABL from as little as 10 pg total RNA (i.e., single cell levels of RNA); in brief, total RNA was extracted from KYO-1 cells and tested over a range of concentrations in both assays (Fig. S1*D*, bottom). The number of U937 and KYO-1 cells that had positive/negative BCR-ABL amplification in the nested qPCR assay and in the qRT-PCR assay were determined (Fig. S1*D*, right).

To determine whether the ability of nested qPCR to detect BCR-ABL+ and BCR-ABL– cells was comparable to that of fluorescence in situ hybridization (FISH), CD34+CD38-CD90+CD45RA- cells were sorted from three additional CML patient samples (CML11-13; Table S1), and analyzed by nested qPCR (as described above; 200 cells per sample) and by FISH

(briefly, cells were immobilized onto positively-charged slides by cytospin and analyzed by conventional dual-color FISH by Quest Diagnostics; 200 cells were scored per sample), and the number of BCR-ABL- and BCR-ABL+ cells were scored in each assay (Fig. S1*E*). Assessment of whether nested qPCR and FISH resulted in different positive or negative rates was performed using R, a system for statistical computation and graphics (3). Percent of positive and negative rates were arcsine transformed to homogenize the variances followed by one-way analysis of variance (ANOVA) with the Randomized Complete Block Design (n=3 blocks/patients).

Single-cell RNA-Seq Data Analysis. For library construction, cDNAs were diluted to 0.1–0.3 ng/µl and barcoded following the Smart-seq2 protocol using a Nextera XT Index Kit (Illumina). A multiplexed library was generated using a Nextera XT DNA Library Prep Kit (Illumina). The fragment distribution of a typical library is shown in Fig. S1*G*. Before deep sequencing, the amplifiable fraction of the library was quantified using a KAPA Library Quantification Lit (Kapa Biosystems) according to the manufacturer's instructions. Finally, 2x75 bp paired-end deep-sequencing was performed using an Illumina NextSeq 500 instrument.

Raw reads from the RNA-seq experiment were first assessed for their quality using fastqc (version 0.10.1) (http://www.bioinformatics.babraham.ac.uk/projects/fastqc), followed by alignment to the reference human genome (hg19) using tophat (version 2.0.14) (4), with default settings except the parameter read-mismatches was set to 2. The RNA-Seq data have been deposited in the Gene Expression Omnibus under access number GSE81730 (the data are accessible to reviewers through the following link: http://www.ncbi.nlm.nih.gov/geo/query/acc.cgi?token=inyboogsvbqpvwj&acc=GSE81730).
All 283 cells were used for exploratory analysis such as visualization by MDS (Fig. S3*D*). HTseq-count (version 0.6.1p1) (5) was used to quantify gene expression. For differential gene expression analysis (Fig. 1 and Fig. S4), cells with < 500,000 aligned reads or < 2000 expressed genes (at least 1 count per million [CPM]) were excluded, as well as genes expressed in less than 20% of filtered cells, which resulted in 271 cells. RSEM (version RSEM/1.2.11) (6, 7) was used to calculate TPMs (Transcripts Per Million), followed by imputation using scImpute (version 0.0.7) (8) with four clusters per patient. Imputed data was transformed using log2(TPM + 1) followed by differential gene expression analysis using MAST (version 1.6.1) (9) with a mixed model, i.e., BCR-ABL status was included in the model as a fixed effect and patient as a random effect (n=3). Genes with $P < 0.01$ and fold change > 1.5 or < 1/1.5 were considered significant. In addition, differential gene expression analysis for each individual patient (Fig. 1*B*) was also performed using the imputed data with the exact permutation test implemented in the perm package.

The MDS plot of Fig. S3*D* was generated using limma package (10). Heatmap and Venn diagrams were drawn with pheatmap and Vennerable packages, respectively. For the pie chart of Fig. S4*C*, the number of genes in each category was first calculated in each individual cell (see Fig. S4*D*), and then all the cells were combined to obtain the average distribution.

Gene Set Enrichment Analysis (GSEA). Statistical enrichment analysis of PANTHER pathways was performed using PANTHER (version 14.0) (11) using default settings.

Ultra-low Cell Number qRT-PCR. Due to the scarcity of the CMLSC population, it is usually difficult to collect enough cells from a frozen CML patient sample for qRT-PCR. To generate cDNA from ~200 cells, we employed a modified single-cell Smart-seq2 protocol. First, to accommodate the volume of sorted cells (< 0.6 µl), the lysis buffer volume was increased from 4 µl to 8 µl, and the reaction volume was doubled in all subsequent steps. Second, rather than using 20 rounds post-amplification cycles for single-cell cDNA synthesis, only 15 rounds were used for 200 cells. To ensure all qRT-PCR experiments were carried out under the same conditions, the method was not only used for analysis of *PIM2* expression in CD34+CD38-CD90+ CMLSCs

(Figs. 2*A*, *E* and *F*) and CD34+CD38- CMLSCs (Fig. S7*F*), but also in CML progenitor (CD34+CD38+) cells (Fig. 2*A*), and mouse CML LSK cells (Figs. S5*C* and S7*G*) and LT-HSCs (Fig. S5*D*). *PIM2* expression was analyzed using primers listed in Table S2.

CML Patient Sample Culturing for Functional Experiments. Cell pellets were re-suspended in binding buffer (1x PBS with 0.2% BSA and 2 mM EDTA) to enrich for bulk live cells or CD34+ cells alone. Cells were then cultured in IMDM medium plus 20% BSA, insulin and transferrin (BIT) (STEMCELL Technologies) and the following cytokines: 100 ng/ml SCF, 100 ng/ml G-CSF, 20 ng/ml FLT3L, 20 ng/ml IL-3, and 20 ng/ml IL-6 (all from ProSpec). For IM-induced apoptosis and cell viability experiments, cells were cultured in the presence of cytokines for 24 h, then cells were switched to IMDM plus 20% BIT with less than 10% of cytokines for the rest of culturing. From our FACS analysis (see Fig. S1*A*), we found that the HSC population (CD34+CD38-CD90+CD45RA-) was almost exclusively CD34+CD38-CD90+, which has also been used previously to define HSCs (12). We therefore used CD34+CD38-CD90+ cells as an alternative for CMLSCs in subsequent phospho-flow, cell viability, apoptosis experiments for convenient FACS analysis.

Phospho-Flow Analysis. Human primary CD34+ cells were cultured for 2 days to expand the population, and then IM-sensitive CML progenitor cells (CD34+CD38+) and IM-resistant CMLSCs (CD34+CD38- and CD34+CD38-CD90+) were FACS sorted using a BD FACSAria II flow cytometer (BD Biosciences) with FACSDIVA software and further cultured for ~16 h in the presence of DMSO, IM (ChemieTek; 5 μM), AZD1208 (Active Biochem; 5 μM) or LGH447 (Selleckchem; 5 μM). K562 cells (ATCC) were cultured for ~16 h in the presence of DMSO, IM (5 μM), or AZD1208 (5 μM). Cells were then collected, fixed, and processed as previously described (13) for staining of PE-conjugated phospho-BAD (S112) (cat. no. 11865, clone 40A9) and PE-conjugated rabbit IgG (cat. no. 5742, clone DA1E) (both from Cell Signaling Technology). To assess efficient inhibition of BCR-ABL activity by IM, K562 or FACS sorted CMLSCs, were treated for 4 h with DMSO or IM (5 μM), and then processed as above and stained with Alexa Fluor 488-conjugated pCRKL antibody (BD Biosciences, cat. no. 560789, clone K30-391.50.80) and Alexa Fluor 488-conjugated IgG (BD Biosciences, cat. no. 557703, clone G155-178). Fixed cells were used either immediately, or stored at 4°C for two weeks.

Immunoblot Analysis. For the experiments in Figs. S7*B* and *C*, K562 cells were treated with 0, 2, 5 or 10 μM pimozide (Calbiochem) (B) or 10 μM IM (C). For the experiments in Fig. S7*D* and *E*, Ba/F3-BCR-ABL cells were generated by transducing Ba/F3 (originally purchased from ATCC) cells with a lentiviral vector expressing doxycycline-inducible BCR-ABL (constructed by replacing the shRNA cassette and TurboRFP reporter in pTRIPZ [GE Dharmacon] with BCR-ABL[p210]). Cells were maintained in RPMI plus 10% fetal bovine serum in the presence of 1 μg/ml doxycycline (Sigma). To assay PIM2 levels upon BCR-ABL or STAT inhibition, Ba/F3-BCR-ABL cells were subjected to doxycycline withdrawal, or treatment with 0, 5 or 10 μM pimozide (D) or 5 μM IM (E). After ~16 h of treatment, protein extracts were prepared and analyzed by immunoblotting for PIM2 (human PIM2: Cell Signaling Technology, cat. no. 4730, clone D1D2; mouse PIM2: Santa Cruz, sc-13514, clone 1D12) and ACTB (Sigma, cat. no. A2228, clone AC-74).

For the experiment shown in Fig. S8*B*, KCL22 cells (obtained from DSMZ) were treated with 0, 0.1, 0.5 or 1 μM IM for 12 h, and protein extracts were analyzed by immunoblotting using a phospho-c-Abl, phospho-Stat5 and phospho-CRKL multiplex western detection cocktail (PathScan, Cell Signaling Technology, cat. no. 5300). For the experiment shown in Fig. S9*J*, K562 and K562R cells (kindly provided by Nicholas J. Donato, University of Michigan) were treated with 1 μM IM or 10 μM AZD1208 for 4 h, and protein extracts were analyzed by immunoblotting for phospho-BAD(Ser112) (Cell Signaling Technology, cat. no. 9291), and BAD

(Cell Signaling Technology, cat. no. 9239, clone D24A9). For the experiment shown in Fig. S10*D*, extracts were prepared from KCL22 cells ectopically expressing PIM1, PIM2 or PIM3 (see below for details) and analyzed by immunoblotting for PIM1 (Cell Signaling Technology, cat. no. 3247, clone C93F2), PIM2 (Cell Signaling Technology, cat. no. 4730, clone D1D2), or PIM3 (Cell Signaling Technology, cat. no. 4165, clone D17C9).

ShRNA-Mediated Knockdown. For knockdowns in CMLSCs (CD34+CD38-CD90+), bulk live cells from frozen CML specimens were enriched using a Dead Cell Removal Kit (Miltenyi Biotec) and cultured overnight at 37°C. For single PIM1, PIM2, PIM3 or STAT4 knockdowns, cells were transduced with a pLKO-GFP lentivirus (constructed by excising the puromycin-resistance gene from pLKO.1 [Addgene plasmid #10878] and replacing it with PCR-amplified GFP) carrying either a control non-silencing shRNA, or human PIM1 (TRCN0000010115), PIM2 (TRCN0000001629 or TRCN0000001630), PIM3 (TRCN0000037414), or STAT4 (TRCN0000020897 or TRCN0000020898) shRNA using two rounds of spin infection, with ~12-16 h in between. For the triple PIM knockdown, the U6-shRNA cassettes for the PIM1 and PIM3 shRNAs were PCR amplified (using primers listed in Table S2) and tandemly assembled via Gibson assembly into the SacII site of the pLKO.1-GFP-PIM2 shRNA vector (carrying TRCN0000001629). For the STAT5A/5B double knockdown, the U6-shRNA cassette for the STAT5B shRNA (TRCN0000019355) was PCR amplified (using primers listed in Table S2) and cloned into the SacII site of a pLKO.1-GFP-STAT5A shRNA vector (carrying TRCN0000019307) using one-step Gibson assembly. For the STAT4/5A/5B triple knockdown, the U6-shRNA cassettes for the STAT5A and STAT5B shRNAs were PCR amplified (using primers listed in Table S2) and tandemly assembled via Gibson assembly into the SacII site of the pLKO.1-GFP-STAT4 shRNA vector (carrying TRCN0000020898). Cells were further cultured for 24 h to allow for expression of the shRNA(s). Cells were treated with IM (5 μM) for an additional 24 h for apoptosis analysis or 48 h for cell viability determination. Knockdown efficiencies for *PIM1*, *PIM2*, *PIM3*, *STAT4*, and *STAT5A/5B* shRNAs were determined in CD34+ CML cells. Following two rounds of spin infection, cells were further cultured for 48 h and then FACS sorted to isolate GFP+ CD34+ cells and GFP- CD34+ cells. Knockdown efficiency was determined by comparing target gene expression between GFP+ and GFP- cells.

For stable single knockdowns in K562 cells or KCL22 cells, 2 x 10^5 cells were seeded in a six-well plate with 1 ml growth medium supplemented with 1 ml lentiviral particles expressing a STAT1 (TRCN0000004266 or TRCN0000004268), STAT2 (TRCN0000007461 or TRCN0000007464), STAT4 (TRCN0000020897 or TRCN0000020898), STAT5A (TRCN0000019304 or TRCN0000019307), STAT5B (TRCN0000019355 or TRCN0000019356), PIM1 (TRCN0000010115), PIM2 (TRCN0000001630), or PIM3 (TRCN0000037414) shRNA. For double or triple knockdowns, 1 x 10^6 cells were resuspended in growth medium (1 ml for double knockdowns and 1.5 ml for triple knockdowns) and co-infected with equal volumes (0.5 ml) of each viral supernatant (for the STAT genes, the following shRNAs were used: STAT4, TRCN0000020898; STAT5A, TRCN0000019307 and STAT5B, TRCN0000019355) at a high MOI (> 500). Cells were spun in the presence of 10 μg/ml polybrene (Sigma Aldrich) at 2500 x g at room temperature for 90 minutes and incubated at 37°C with 5% CO_2 for 3 h; for double and triple knockdowns, the spin infection was repeated on the following day. Following the spin infection, 2 ml of fresh growth media was added and the cells were allowed to grow for 16 h. Cells were then spun down, washed with PBS, resuspended in 2 ml of fresh media, and subjected to puromycin selection (2 μg/ml) for 4 days. For IM treatment, 2 x 10^6 KCL-22 cells stably expressing an shRNA were cultured in the presence of IM (1 μM) for 12 h, and conventional qRT-PCR was performed to analyze expression of *PIM2* or the target gene (see Table S2 for primer sequences).

Datamining. GEO2R (accessed on 2/22/18) (https://www.ncbi.nlm.nih.gov/geo/info/geo2r.html) was used for microarray data mining from the published GEO datasets GSE43754 (14), GSE43225 (15), and GSE20876 (16). R packages GEOquery (http://www.bioconductor.org/packages/2.8/bioc/html/GEOquery.html) and limma (http://www.bioconductor.org/packages/release/bioc/html/limma.html) (17) were used for differential gene expression analysis in GEO2R. For analysis of *PIM2* expression (Fig. S7*I* and *J*), the expression value of *PIM2* from untreated and IM-treated samples was extracted from GSE43225 and GSE20876, and plotted. For analysis of *STAT* gene expression (Fig. S8*A*), the expression values of *STAT* genes were extracted from GSE43754, and relative expression of *STAT* genes was determined by normalizing individual gene expression in CMLSCs to that in CML progenitors.

ChIP. ChIP assays were performed as previously described (18) in KCL22 cells treated in the presence or absence of 1 μM IM (12 h) using phospho-STAT4(Tyr693) (Cell Signaling Technology, cat. no. 4134, clone D2E4) or phospho-STAT5(Tyr694) (Cell Signaling Technology, cat. no. 9351) antibodies. ChIP products were analyzed by qPCR using primers as listed in Table S2. Fold enrichment was calculated by comparing signal enrichment between the antibody pull-down DNA and the normal rabbit IgG control, and then normalized to background enrichment at a downstream region located within exon 5 of *PIM2*, which was set to 1.

Relative Cell Viability and Apoptosis Assays. For the experiments shown in Fig. 3, bulk primary human cells were stained with PE-cy7-conjugated CD34 (eBioscience, cat. no. 25-0349, clone 4H11), APC-conjugated CD38, and PE-conjugated CD90 antibodies, Pacific Blue-conjugated Annexin V, and 7-AAD, and immediately analyzed by FACS. For relative cell viability, the percentage of the HSC fraction was determined by FACS analysis, and the total cell number was determined by trypan blue cell counting. The number of viable cells was determined as [Total viable cell number] x [percentage of CMLSCs]. For mouse CML LSK cells (Fig. 4*B* and *C*), apoptosis and viability were determined as previously described (13). For analysis of mouse ST-HSCs and LT-HSCs (Fig. 4*D*), total mouse bone marrow cells were stained with a cocktail of primary antibodies [APC-conjugated Sca-1 (cat. no. 17-5981, clone D7), PE-conjugated c-Kit (cat. no. 12-1171, clone 2B8), Pacific blue-conjugated CD48 (cat. no. 48-0481, clone HM48-1), PE-cy7-conjugated CD150 (cat. no. 25-1502, clone mShad150) antibodies (all from eBioscience), and Biotin-conjugated Lineage antibody cocktail (Miltenyi Biotec, cat. no. 130-092-613)], followed by staining with APC-eFluor780-conjugated streptavidin secondary antibody (eBioscience; cat. no. 47-4317) as previously described (13). Representative staining is shown in Fig. S5*A*. After initially culturing for 24 h, cells were treated with DMSO, IM (5 μM), AZD1208 (5 μM) or a combination of IM and AZD1208 for 24 h for apoptosis analysis or 48 h for cell viability determination. For the experiments shown in Fig. S9*D* and *E*, cells were treated with DMSO, IM (5 μM), LGH447 (5 μM) or a combination of IM and LGH447 for 16 h for cell viability determination. For the experiment shown in Fig. S9*I*, K562R cells were treated with DMSO, IM (1 μM), AZD1208 (1 μM) or a combination of IM and AZD1208 for 48 h prior to cell viability determination by MTT. For the experiment shown in Fig. S9*K*, primary CML cells from IM-resistant patients harboring wild-type BCR-ABL (n=3; CML8-10; Table S1) were treated with DMSO, IM (5 μM), AZD1208 (5 μM) or a combination of both drugs for 48 h prior to cell viability determination by trypan blue cell counting.

For the experiments shown in Figs. S9*H* and S10*E*, KCL22 cells were treated with DMSO, IM (1 μM), AZD1208 (1 μM in Fig. S9*H* and 0.1 μM in Fig. S10*E*) or a combination of IM and AZD1208 for 72 h prior to cell viability determination using PrestoBlue Cell Viability Reagent (Invitrogen) as per the manufacturer's instructions. For the experiment shown in Fig. S10*C*, KCL22 cells were treated with DMSO or IM (1 μM) for 40 h prior to cell viability determination using PrestoBlue Cell Viability Reagent.

Ectopic PIM Expression. To generate PIM overexpression vectors, PIM1, PIM2 and PIM3 were PCR amplified from cDNA templates (PIM1, OHu28516D and PIM3, OHu28503D from GenScript; and PIM2, ID: 3913552 from the MGC cDNA library) (using primers listed in Table S2) and cloned into the lentiviral vector pHR_PGK (Addgene plasmid #79120), which contains IRES-puro. For the PIM1/2/3 triple overexpression vector, PIM1, PIM2 and PIM3 were PCR amplified from the cDNA templates mentioned above (using primers listed in Table S2) and assembled in pHR_PGK via Gibson assembly. The vectors were packaged into lentiviral particles and used to transduce KCL22 cells, which were subjected to puromycin selection (1 μg/ml) for 10 days.

Colony Formation Assays. For colony formation assays, ~500 CD34+ cells or bulk cells with equivalent number of CD34+ cells (obtained from CML patient sample CML1; Table S1) were plated on 35 mm dishes in MethoCult H4435 Enriched medium supplemented with recombinant human cytokines (STEMCELL Technologies), and treated with DMSO, IM (5 μM), AZD1208 (5 μM) or a combination of IM and AZD1208. Total colonies were counted at day 14.

PDX Mice. Animal protocols were approved by the Institution Animal Care and Use Committee at UMMS (A-262). Animal sample sizes were selected based on precedent established from previous publications and an understanding that at least n=5 is generally required to achieve statistical significance. Mice were randomly allocated to each group for drug treatment after engraftment, and were subsequently analyzed in a non-blinded fashion. No animals were excluded from the study.

CD34+ cells were enriched from a human CML sample obtained from a newly diagnosed patient (CML1; Table S1) by positive selection using CD34 magnetic selection beads (Miltenyi Biotec). CD34 purity levels were confirmed by flow cytometry using anti-human CD34 (clone 561) and anti-human CD45 (clone HI30) antibodies from BioLegend. $1x10^6$ CD34+ cells were injected intravenously into two male 10-week old recipient immunodeficient NSG-SGM3 mice (The Jackson Laboratory) 4 h after the mice were irradiated with 100 cGy, and the engraftment was allowed to proceed for 81 days.

To ensure successful engraftment, peripheral blood was analyzed for human CD45+ by flow cytometry. In brief, whole blood was collected from engrafted NSG-SGM3 mice in heparin, and 75 μl of blood was washed with FACS buffer (PBS with 2% FBS and 0.02% sodium azide). Blood samples were incubated with rat anti-mouse CD16/CD32 (clone 2.4G2, BD Biosciences) for 5–7 min at 4°C to block Fc binding, and then incubated with an antibody against human CD45 for 20 minutes at 4°C. Samples were then treated with BD FACS Lysing Solution (BD-Biosciences) to lyse red blood cells and fix the cells. At least 20,000 events were collected on a BD Accuri C6 flow cytometer (BD Biosciences) for analysis. 3.25% and 13.6% of human CD45+ cells were detected in the peripheral blood of the two mice, indicating successful engraftment.

The two NSG-SGM3 mice were sacrificed, and CD34+ cells were isolated from splenocytes and bone marrow using the positive selection approach described above and pooled. Secondary recipient NSG-SGM3 mice were irradiated with 100 cGy and injected intravenously with $1x10^6$ CD34+ cells 4 h after irradiation. Approximately two weeks after engraftment, healthy secondary recipients aged 7-17 weeks were treated with vehicle (n=5 mice, all male), IM (100 mg/kg, twice a day; n=5 mice, 4 males and 1 female), AZD1208 (30 mg/kg, once a day; n=5 mice, 4 males and 1 female), or a combination of IM and AZD1208 (n=5 mice, 3 males and 2 females). Treatments were terminated when human CD45+ cells reached at least 22% in peripheral blood of the control mice (approximately 11 weeks). All mice were sacrificed, and the presence of human bulk CML cells (CD45+) in peripheral blood and spleen, and the presence of CML cells (CD34+) and CMLSCs (CD34+ CD38- CD90+) in the spleen, were determined by FACS analysis using anti-human CD45 (clone HI30), anti-human CD34 (clone 561), anti-human CD38 (clone HB-7) and anti-human CD90 (clone 5E10) antibodies from BioLegend. At least

50,000 events were collected on BD LSR-II flow cytometer (BD Biosciences) for analysis. Data were analyzed using FlowJo software (Tree Star, Inc.).

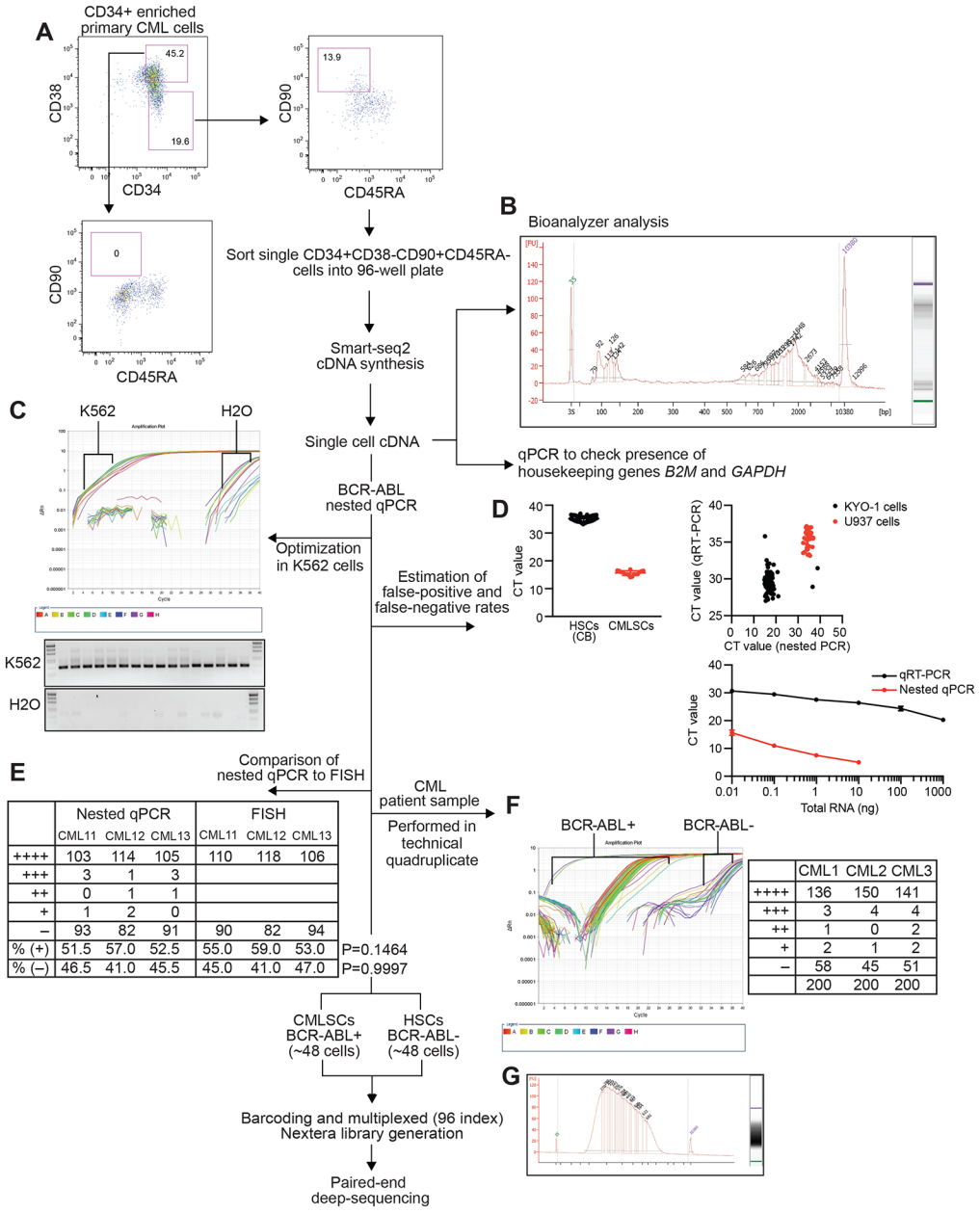

	Nested qPCR			FISH			
	CML11	CML12	CML13	CML11	CML12	CML13	
++++	103	114	105	110	118	106	
+++	3	1	3				
++	0	1	1				
+	1	2	0				
–	93	82	91	90	82	94	
% (+)	51.5	57.0	52.5	55.0	59.0	53.0	P=0.1464
% (–)	46.5	41.0	45.5	45.0	41.0	47.0	P=0.9997

	CML1	CML2	CML3
++++	136	150	141
+++	3	4	4
++	1	0	2
+	2	1	2
–	58	45	51
	200	200	200

Fig. S1. Single-cell RNA-seq workflow. (*A*) Primary CML patient samples were enriched for CD34+ cells using magnetic beads. Enriched CD34+ cells were stained with CD34, CD38, CD90, and CD45RA cell surface markers, and single CD34+CD38-CD90+CD45RA- cells were collected and converted into cDNA using a revised Smart-seq2 protocol. (*B*) cDNA quality was checked on a Bioanalyzer; a representative single cell cDNA size distribution is shown. qPCR was performed to detect the expression of housekeeping genes *B2M* and *GAPDH*. (*C*) Because the expression level of BCR-ABL is typically low in primary CML cells, particularly in the stem cell population from chronic phase CML patients, nested qPCR was performed to enhance specificity and sensitivity for detection of BCR-ABL. Nested qPCR for BCR-ABL was first optimized in human CML K562 cells. Briefly, cDNAs were prepared from 16 single K562 cells and, following confirmation of expression of housekeeping genes, two-step nested qPCR was carried out to detect BCR-ABL. The inset on the bottom left shows that all 16 single K562 cells

showed positive amplification (> 1,000-fold over background) with no detectable signal in the water (H2O) control, confirming the validity of this approach. (*D*) Estimation of false-positive and false-negative rates of the nested qPCR assay. (Left) Results of nested qPCR for BCR-ABL in 48 HSCs (CD34+CD38-CD90+CD45RA-) or, as a positive control, 16 CMLSCs (CD34+CD38-CD90+CD45RA-) that had been previously identified as BCR-ABL+ by the nested qPCR assay. The results show that none of the 48 BCR-ABL- CD34+CD38-CD90+CD45RA- cells showed positive BCR-ABL amplification, whereas all 16 BCR-ABL+ CMLSCs showed positive amplification. The results indicate that the false-positive rate was very low: less than 1 in 48, or < 2%. (Right) Nested qPCR and qRT-PCR analysis of 40 single BCR-ABL- human lymphoblast U937 cells and 94 single BCR-ABL+ human CML KYO-1 cells. Analysis of the assays using total RNA isolated from KYO-1 cells confirmed that each assay was sensitive enough to detect BCR-ABL from as little as 10 pg of total RNA (i.e., single cell levels of RNA) (bottom; error bars indicate SD; n=3 technical replicates of a single experiment. The results (top, right) show that all 40 BCR-ABL- U937 cells failed to show positive BCR-ABL amplification in the nested qPCR assay, consistent with the finding above that the false-positive rate of the nested qPCR assay is very low (less than 1 in 40, or < 2.5%). By contrast, 2 of the 94 BCR-ABL+ KYO-1 cells failed to show positive BCR-ABL amplification in the nested qPCR assay, despite showing positive amplification in the gene-specific qRT-PCR assay, indicating the nested qPCR assay had a false-negative rate of 2.1%. The results also show that compared to the BCR-ABL-specific qRT-PCR assay, nested qPCR yields a much stronger positive signal and shows a distinct separation of BCR-ABL+ cells from BCR-ABL- cells. (*E*) Comparison of the ability of nested qPCR and FISH to detect BCR-ABL+ and BCR-ABL- cells. CD34+CD38-CD90+CD45RA- cells sorted from each of three CML patient samples (CML11-13; Table S2) were analyzed by nested qPCR or FISH to detect BCR-ABL. For nested qPCR, each cell was tested in technical quadruplicate, and samples were scored as being BCR-ABL-positive in all four replicates (++++), three replicates (+++), two replicates (++), one replicates (+) or no replicates (–, or BCR-ABL-negative); only single cells that were positive for BCR-ABL in all four replicates were counted as "positive". Statistical analysis revealed that there was no significant difference between the positive rates (P=0.1464) and negative rates (P=0.9997) of the two techniques, indicating that the nested qPCR assay was comparatively accurate to FISH in determining the BCR-ABL status of a cell. (*F*) Nested qPCR was then performed for single CD34+CD38-CD90+CD45RA- cells from CML patients. For every plate of single cells (~96 cells), 16 water control samples were also included; if any of the water controls was positive, the nested qPCR was discarded and repeated. The BCR-ABL signal in single cells had a ~1,000-fold reduced intensity compared to control K562 cells; a typical amplification from a plate of single cells is shown. Each single cell was tested in technical quadruplicate, and samples were scored as being BCR-ABL-positive in all four replicates (++++), three replicates (+++), two replicates (++), one replicates (+) or no replicates (–, or BCR-ABL-negative). For each sample, we analyzed ~200 single cells and could obtain ~135-150 cells (~70-75%) that showed a positive BCR-ABL signal in all four replicates, and ~45-60 cells that were negative for BCR-ABL in all four replicates (inset table). Only single cells that were either positive or negative for BCR-ABL in all four replicates were selected for further analysis by RNA-seq. (*G*) Finally, ~96 BCR-ABL+ and BCR-ABL- CD34+CD38-CD90+CD45RA- cells were combined to generate a cDNA library for deep-sequencing; a representative 96 index cDNA library size distribution is shown.

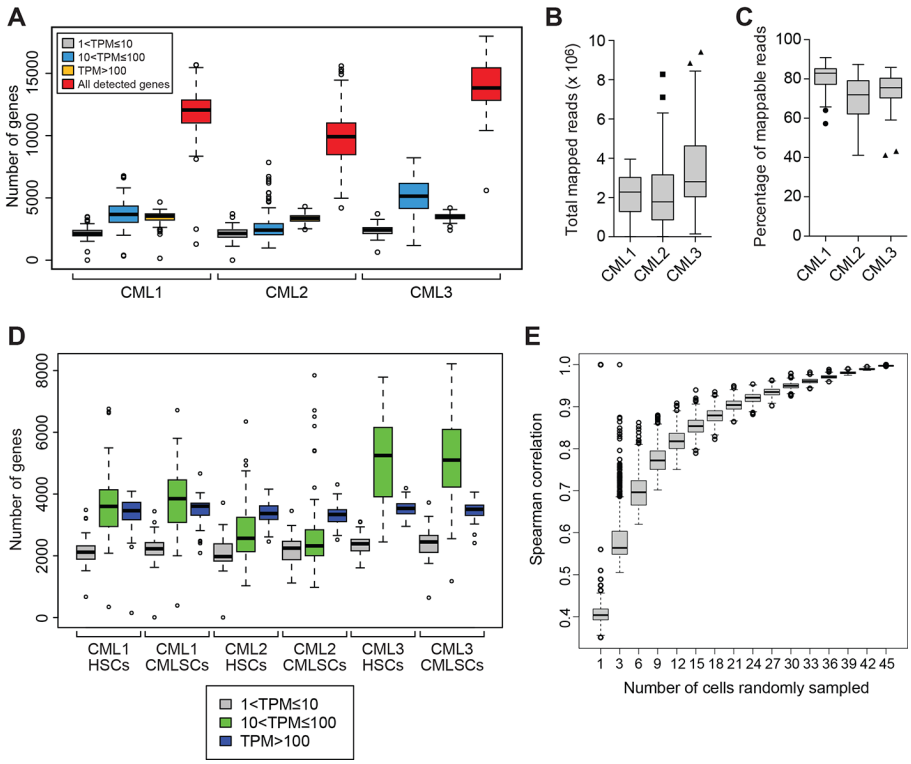

Fig. S2. Quality controls for single-cell RNA-seq data. (*A*) Number of genes expressed at a low ($1 < TPM \leq 10$), modest ($10 < TPM \leq 100$), or high ($TPM > 100$) level in single CMLSCs and HSCs isolated from three CML patients. Error bars indicate SD; n=~96 biological replicates. (*B* and *C*) Box plots showing the number of total mapped reads (B) or the percentage of mappable reads (C) in all single HSCs and CMLSCs (CD34+CD38-CD90+CD45RA-) from each CML sample. Boxed areas span the first to the third quartile, and whiskers represent maximum or minimum observations within 1.5 inter-quartile range (IQR). (*D*) Number of genes expressed at a low ($1 < TPM \leq 10$), modest ($10 < TPM \leq 100$), or high ($TPM > 100$) level across all single cells in each patient. The results from BCR-ABL+ and BCR-ABL- CD34+CD38-CD90+CD45RA- cells are presented separately. Error bars indicate SD; n=~48 biological replicates. (*E*) Box plot showing the distribution of the Spearman correlation coefficient of the global transcription profile of an increasing number of randomly sampled HSCs (CD34+CD38-CD90+CD45RA-) from the CML1 patient sample. The results show that the correlation reaches above 0.9 at ~30 cells. Boxed areas span the first to the third quartile, and whiskers represent maximum or minimum observations within 1.5 IQR.

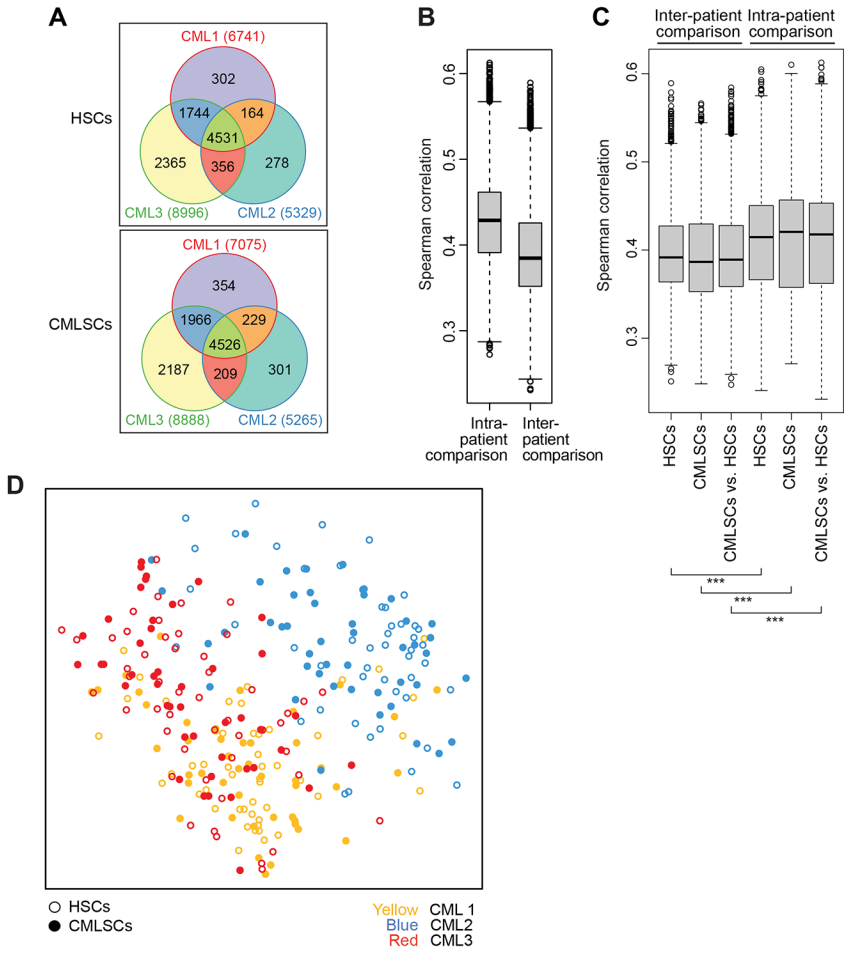

Fig. S3. Substantial differences and heterogeneity in HSC and CMLSC gene expression patterns among the three CML patients. (*A*) Venn diagrams showing the number of common detectable genes in HSCs and CMLSCs (CD34+CD38-CD90+CD45RA-) from three CML patients. A detectable gene is defined as one with TPM > 1 in more than 50% of single cells. (*B*) Box plot showing the distribution of the Spearman correlation coefficient of the global transcription profile of every pair-wise combination of single cells within the same patient (intra-patient correlation) and between any pair of cells from different patients (inter-patient correlation). HSCs and CMLSCs were analyzed separately and then combined. Boxed areas span the first to the third quartile, and whiskers represent maximum or minimum observations within 1.5 inter-quartile range (IQR). $P < 0.001$. (*C*) Box plot showing the distribution of the Spearman correlation coefficient of the global transcription profile of every pair of single cells within the same patient (intra-patient correlation) and between any pair of cells from different patients (inter-patient correlation). The results from BCR-ABL+ and BCR-ABL- CD34+CD38-CD90+CD45RA- cells were analyzed separately. Boxed areas span the first to the third quartile, and whiskers represent maximum or minimum observations within 1.5 IQR. The results of (B) and (C) show that the inter-patient correlation was significantly lower than the intra-patient correlation, indicating there was greater heterogeneity between CML patients than between CMLSCs and HSCs of the same patient. ***$P < 0.001$. (*D*) Multidimensional scaling plot showing the inter-relationship of gene expression profiles of 283 single HSCs and CMLSCs from three CML patients. The distance between any two cells reflects the similarity of their expression profiles. The results confirm there was greater heterogeneity between CML patients than between CMLSCs and HSCs of the same patient.

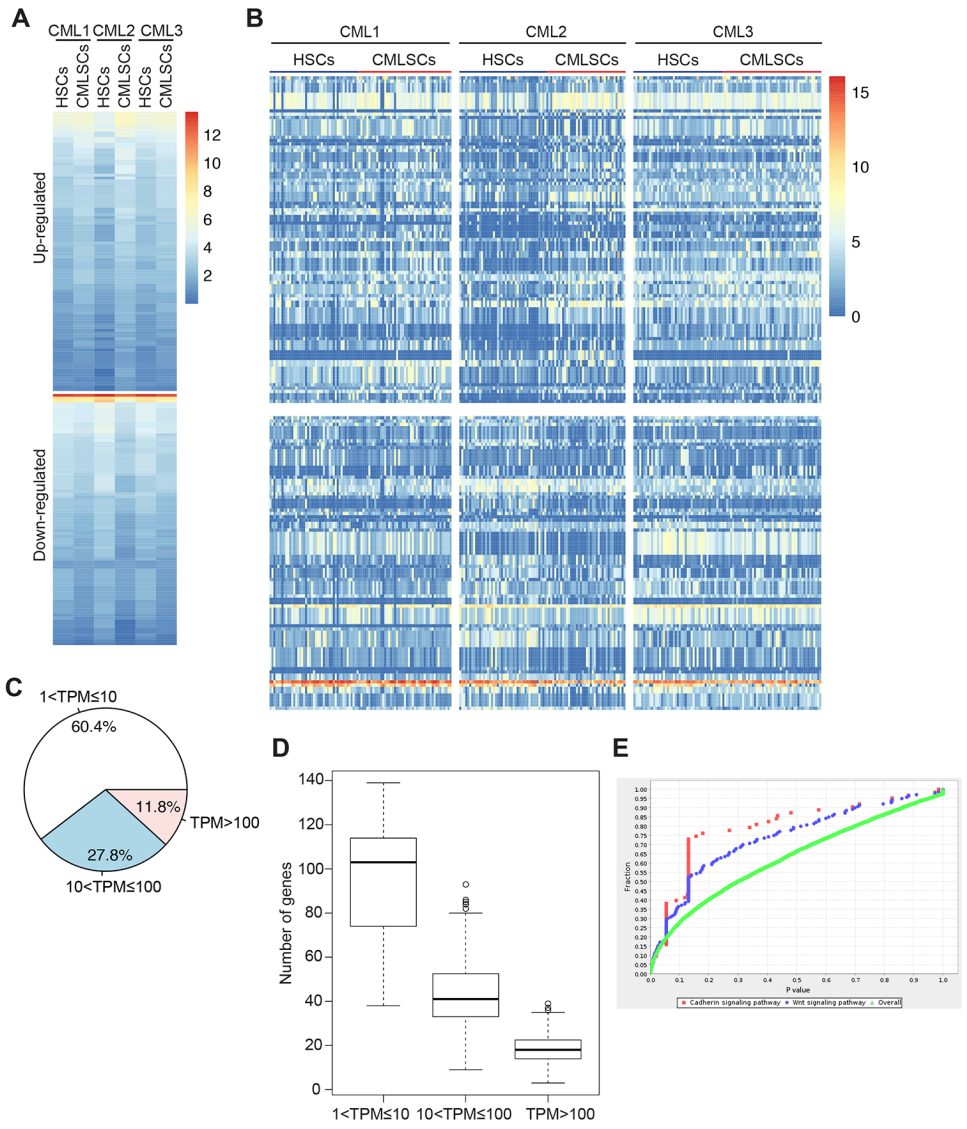

Fig. S4. Gene expression patterns and statistics in single cells. (*A*) Heatmap showing the population average of differentially expressed genes between all single HSCs (BCR-ABL- CD34+CD38-CD90+CD45RA-) and CMLSCs (BCR-ABL+ CD34+CD38-CD90+CD45RA-) in three CML patients. Only those differentially expressed genes with adjusted $P < 0.01$ and fold change > 1.5 or < 1/1.5 are shown. (*B*) Heatmap showing the differentially expressed genes of 271 individual single HSCs and CMLSCs in three CML patients. Only those differentially expressed genes with $P < 0.01$ and fold-change > 1.5 or < 1/1.5 are shown. (*C*) Pie chart showing the average distribution of differentially expressed genes at low ($1 < TPM \leq 10$), modest ($10<TPM\leq100$), and high ($TPM > 100$) levels in all single cells. (*D*) Box plot showing the distribution of the number of differentially expressed genes ($P < 0.01$ and fold change > 1.5 or < 1/1.5) at a low ($1 < TPM \leq 10$), modest ($10 < TPM \leq 100$), or high ($TPM > 100$) level in all single CD34+CD38-CD90+CD45RA- cells. Boxed areas span the first to the third quartile, and whiskers represent maximum or minimum observations within 1.5 IQR. (*E*) GSEA analysis output.

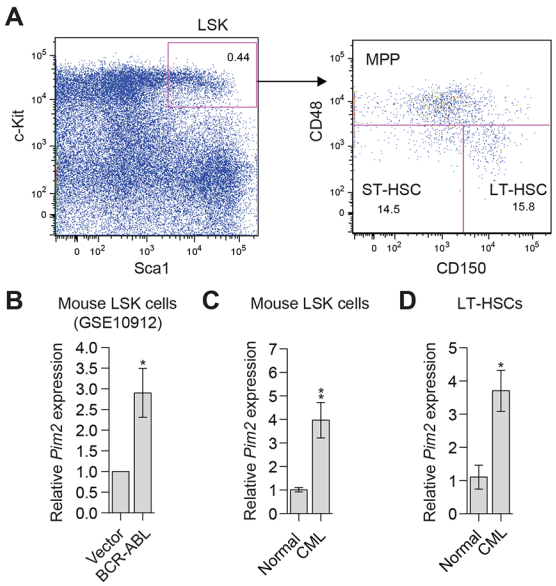

Fig. S5. *Pim2* expression is elevated in mouse CMLSCs. (*A*) FACS plot showing the gating of murine Lin-Sca1+Kit+ (LSK) cells, multi-potent progenitor (MPP, LSKCD48+CD150-) cells, short-term HSCs (ST-HSC, LSKCD48-CD150-), and long-term HSCs (LT-HSC, LSKCD48-CD150+) derived from the inducible BCR-ABL transgenic mouse model. (*B*) qRT-PCR analysis showing relative *Pim2* mRNA levels in murine LSK cells expressing vector or BCR-ABL; the data were mined from a published expression profiling study (GSE10912; ref. (19)). Error bars indicate SEM; n=2 biological replicates. (*C*) qRT-PCR analysis showing relative *Pim2* mRNA levels in murine LSK cells from normal mice (Tet-off SCL-tTA/BCR-ABL transgenic mice given tetracycline-water since birth) and CML mice (Tet-off SCL-tTA/BCR-ABL transgenic mice subjected to tetracycline-water withdrawal at 8 weeks of age). Error bars indicate SEM; n=4 mice per group. (*D*) qRT-PCR analysis showing relative *Pim2* mRNA levels in LT-HSCs from control (normal) and BCR-ABL transgenic mice. Error bars indicate SEM; n=3 mice per group. $*P \leq 0.05$, $**P \leq 0.01$.

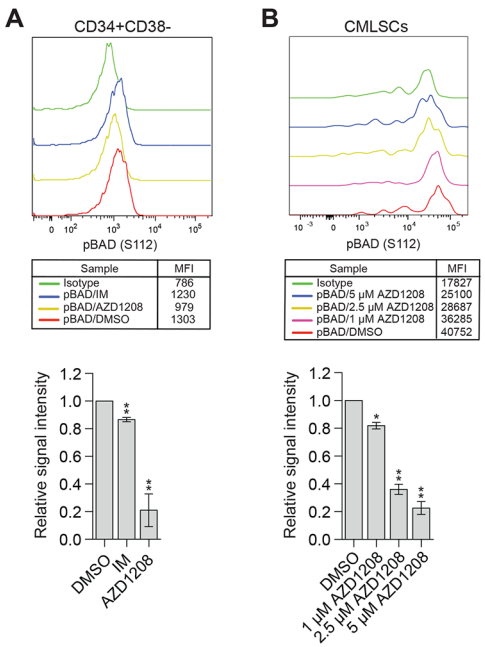

Fig. S6. Treatment with AZD1208 reduces pBAD levels in CD34+CD38- CMLSCs and in CD34+CD38-CD90+ CMLSCs in a dose-dependent manner. (*A* and *B*) Phospho-flow analysis showing intra-cellular staining of pBAD (S112) levels in CD34+CD38- CMLSCs treated with DMSO, IM, or AZD1208 (5 µM) (A), or in CD34+CD38-CD90+ CMLSCs treated with 1, 2.5 or 5 µM AZD1208 (B). IgG was used for control staining. The upper panel shows a representative FACS histogram. The geometric mean fluorescence intensity (MFI) value is indicated in the boxed region. The lower panel shows the quantification of n=3 (A) or n=2 (B) biological replicates. Error bars indicate SEM. *$P \leq 0.05$, **$P \leq 0.01$.

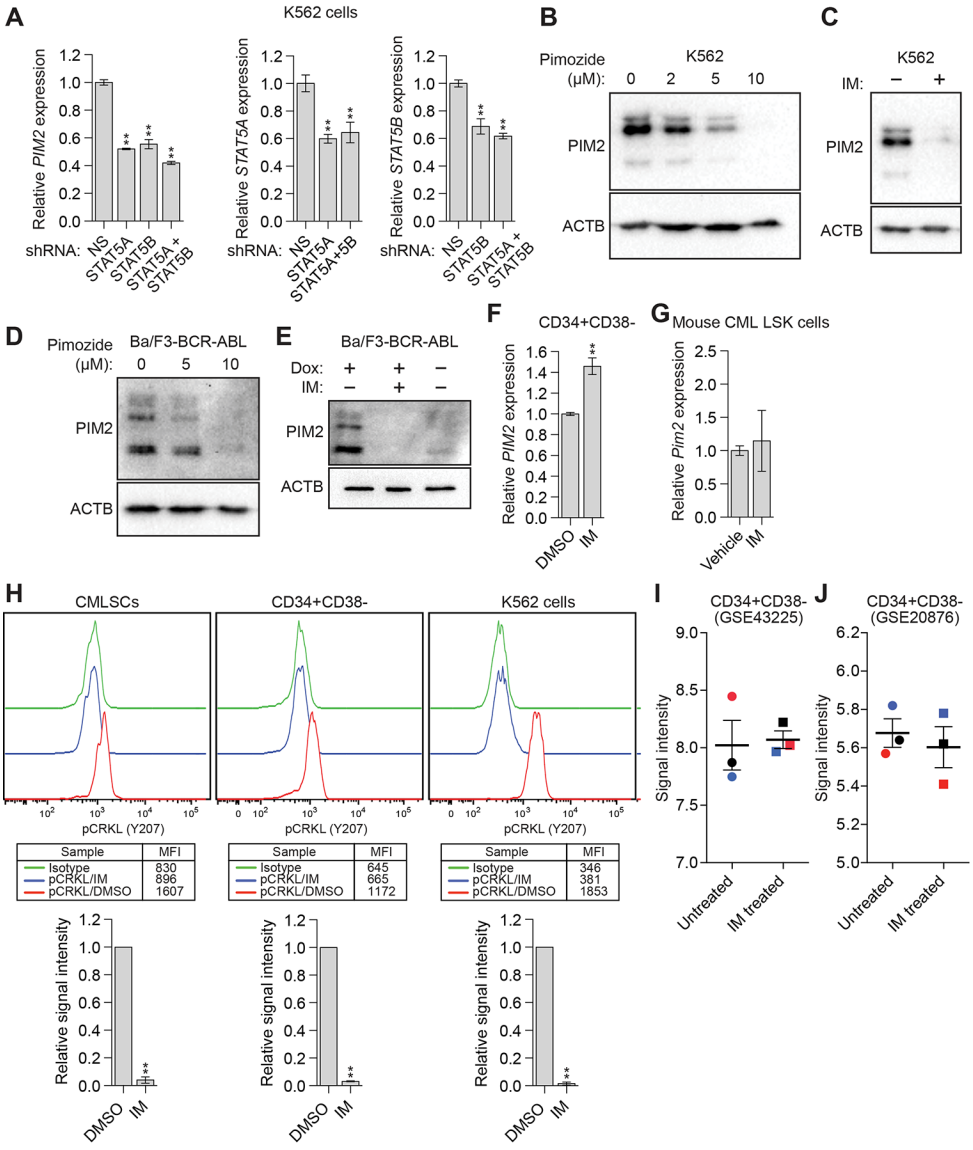

Fig. S7. *PIM2* expression is regulated by BCR-ABL and STAT5 in IM sensitive CML cells, and is not affected by IM treatment in IM-resistant CMLSCs. (*A*, *Left*) qRT-PCR monitoring *PIM2* expression in K562 cells expressing a NS, STAT5A or STAT5B shRNA, or combined STAT5A and STAT5B shRNAs. The results show that shRNA-mediated knockdown of either of the two highly related STAT5 proteins, STAT5A or STAT5B, results in decreased *PIM2* levels. (*A*, *Center and right*) qRT-PCR monitoring knockdown efficiencies of STAT5A (center) and STAT5B (right) shRNAs, expressed in K562 cells either individually or in combination. Error bars indicate SD; n=3 technical replicates of a representative experiment (out of 2 experiments). (*B*) Immunoblot showing PIM2 levels in IM-sensitive K562 cells treated with the small molecule STAT5 inhibitor, pimozide (20). β-actin (ACTB) was monitored as a loading control. The results show that in IM-sensitive CML cells, inhibition of STAT5 phosphorylation/activation resulted in decreased PIM2 levels, demonstrating that PIM2 expression is regulated by STAT5. (*C*) Immunoblot showing PIM2 levels in K562 cells in the absence or presence of IM. The results show that in IM-sensitive CML cells, PIM2 expression depends on BCR-ABL kinase activity. (*D*) Immunoblot showing PIM2 levels in IM-sensitive BCR-ABL-transformed mouse Ba/F3 (Ba/F3-BCR-ABL) cells treated with pimozide. (*E*) Immunoblot showing PIM2 levels in Ba/F3

cells expressing a doxycycline-inducible BCR-ABL fusion protein (Ba/F3-BCR-ABL cells). Cells were maintained in doxycycline (Dox) and subjected to Dox withdrawal or treatment with IM. The results show that PIM2 levels were much higher in Ba/F3-BCR-ABL cells than in parental Ba/F3 cells, and that treatment of Ba/F3-BCR-ABL cells with IM led to a large reduction in PIM2 levels. (*F*) qRT-PCR analysis showing relative *PIM2* mRNA levels in DMSO and IM-treated CD34+CD38- CMLSCs. Error bars indicate SD; n=3 technical replicates of a representative experiment (out of two experiments). (*G*) qRT-PCR analysis showing relative *Pim2* mRNA levels upon IM treatment in LSK cells from CML mice. CML mice were treated with vehicle or IM for two weeks, bone marrow was harvested, and LSK cells were sorted by FACS. Error bars indicate SEM; n=3 mice per group. The results of F and G show that IM treatment of IM-resistant human CMLSCs and mouse CML LSK cells did not significantly reduce *PIM2* levels. (*H*) Phospho-flow analysis showing intra-cellular staining of phosphorylated CRKL (pCRKL) (Y207) levels, a cellular marker of BCR-ABL activity, in CMLSCs (CD34+CD38-CD90+, CD34+CD38-), or as a control K562 cells, treated with DMSO or IM. IgG was used for control staining. The upper panels show representative FACS histograms. The geometric mean fluorescence intensity (MFI) values are indicated in the boxed region. The lower panel shows the quantification of n=3 biological replicates. Error bars indicate SEM. The results confirmed complete inhibition of BCR-ABL activity by IM. (*I* and *J*) Relative *PIM2* mRNA levels in CD34+CD38- CMLSCs treated in the presence or absence of IM. The data were mined from published expression profiling studies GSE43225 (15) (I) and GSE20876 (16) (J). Matched samples from the same patient are indicated by dots of the same color. Error bars indicate SEM; n=3 biological replicates. The results shown that *PIM2* expression is not affected by IM treatment in CD34+CD38- CMLSCs. $*P \leq 0.05$, $**P \leq 0.01$.

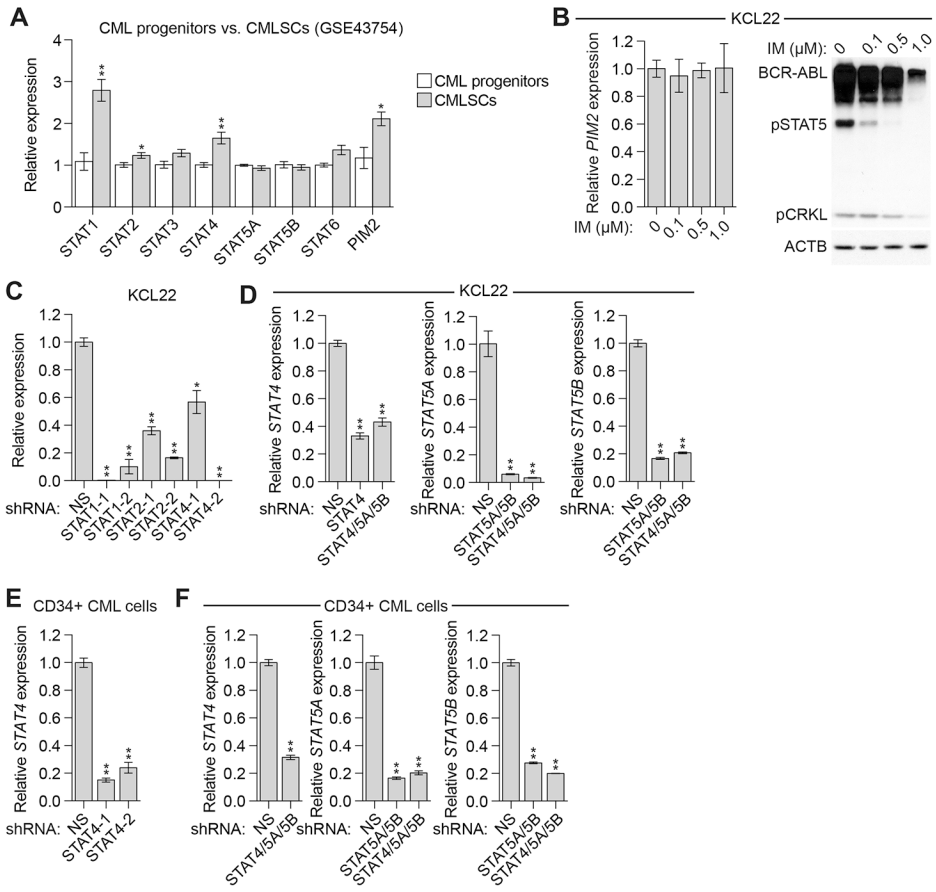

Fig. S8. *PIM2* expression is regulated by both STAT5 and STAT4 in IM-resistant CMLSCs and CML cells. (*A*) Analysis of a published microarray (GSE43754 (14)) showing expression of *STAT* genes in CMLSCs (CD34+CD38-ALDH^{high}) compared to CML progenitors (CD34+CD38+). Error bars indicate SEM; n=5 biological replicates. The results show that *STAT1*, *STAT2* and *STAT4* were significantly upregulated in CMLSCs compared to CML progenitors. As expected, expression of *PIM2* was also higher in CMLSCs compared to CML progenitors. (*B*) qRT-PCR analysis (left) or immunoblot (right) monitoring PIM2 levels in KCL22 cells treated with 0.1, 0.5 or 1 μM IM. Error bars indicate SD; n=3 technical replicates of a representative experiment (out of at least 2 experiments). The results show that expression of PIM2 is not inhibited by IM even at a concentration of 1 μM, which is sufficient to inhibit BCR-ABL signaling, as evidenced by reduced levels of BCR-ABL substrates, pSTAT5 and pCRKL. (*C*) qRT-PCR monitoring knockdown efficiencies of STAT1, STAT2, and STAT4 shRNAs in KCL22 cells. Error bars indicate SD; n=3 technical replicates of a representative experiment (out of 2 experiments). (*D*) qRT-PCR monitoring knockdown efficiencies of STAT4 (*Left*), STAT5A (*Center*) and STAT5B (*Right*) shRNAs, expressed alone or in combination, in KCL22 cells. Error bars indicate SD; n=3 technical replicates of a representative experiment (out of 2 experiments). (*E*) qRT-PCR monitoring knockdown efficiency of STAT4 in CD34+ CML cells. Error bars indicate SD; n=3 technical replicates of a representative experiment (out of 2 experiments). (*F*) qRT-PCR monitoring knockdown efficiencies of STAT4 (*Left*), STAT5A (*Center*) and STAT5B (*Right*) in CD34+ CML cells. Error bars indicate SD; n=3 technical replicates of a representative experiment (out of 2 experiments). *$P \leq 0.05$, **$P \leq 0.01$.

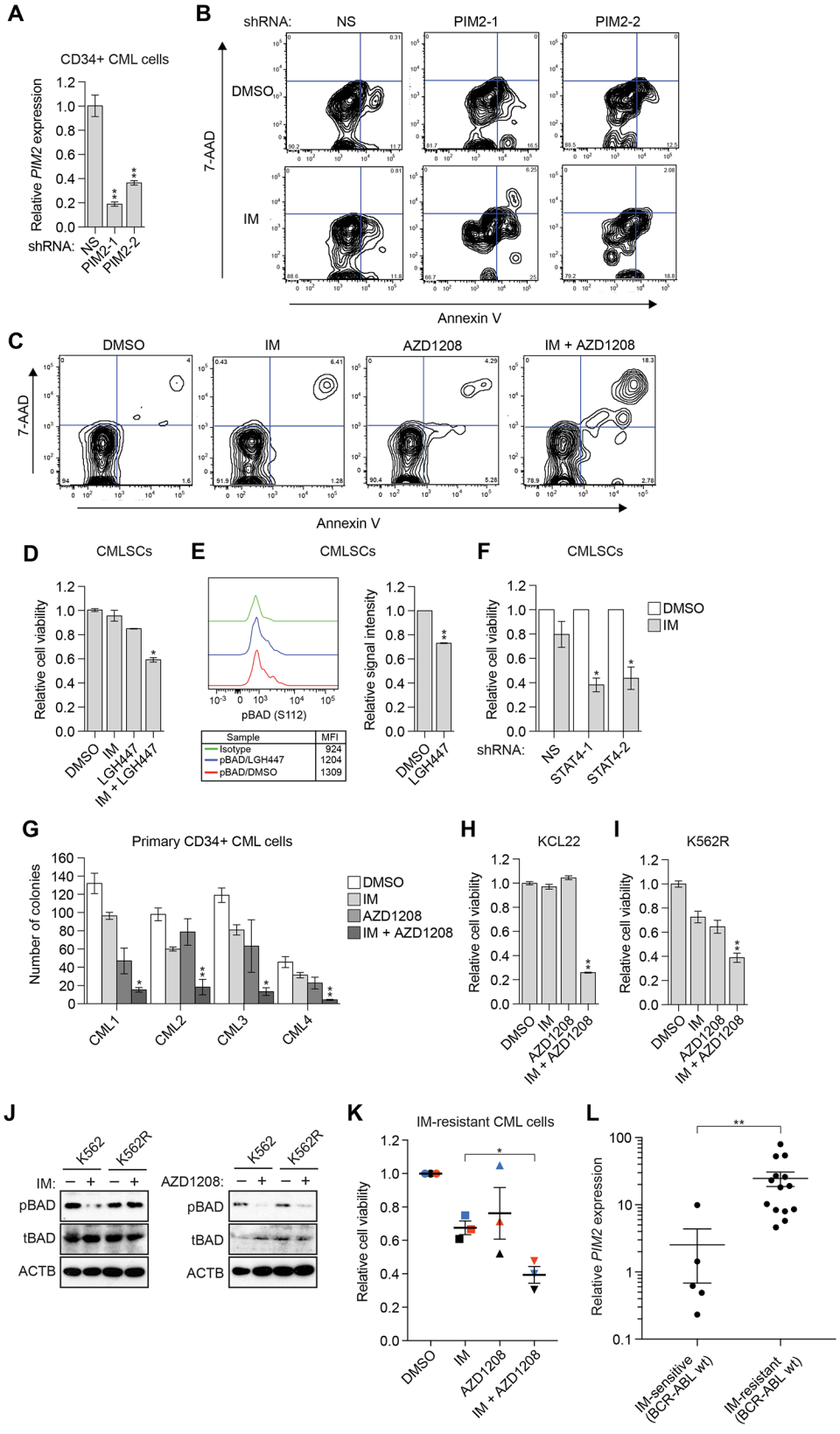
A
CD34+ CML cells
Relative PIM2 expression
shRNA: NS PIM2-1 PIM2-2
B
shRNA: NS PIM2-1 PIM2-2
DMSO
IM
7-AAD
Annexin V
C
DMSO
IM
AZD1208
IM + AZD1208
7-AAD
Annexin V
D
CMLSCs
Relative cell viability
DMSO IM LGH447 IM + LGH447
E
CMLSCs
pBAD (S112)
Sample MFI
Isotype 924
pBAD/LGH447 1204
pBAD/DMSO 1309
Relative signal intensity
DMSO LGH447
F
CMLSCs
Relative cell viability
DMSO
IM
shRNA: NS STAT4-1 STAT4-2
G
Primary CD34+ CML cells
Number of colonies
DMSO
IM
AZD1208
IM + AZD1208
CML1 CML2 CML3 CML4
H
KCL22
Relative cell viability
DMSO IM AZD1208 IM + AZD1208
I
K562R
Relative cell viability
DMSO IM AZD1208 IM + AZD1208
J
K562 K562R
IM: – + – +
pBAD
tBAD
ACTB
K562 K562R
AZD1208: – + – +
pBAD
tBAD
ACTB
K
IM-resistant CML cells
Relative cell viability
DMSO IM AZD1208 IM + AZD1208
L
Relative PIM2 expression
IM-sensitive (BCR-ABL wt)
IM-resistant (BCR-ABL wt)

Fig. S9. Additional experiments related to Figure 3. (*A*) qRT-PCR monitoring knockdown efficiencies of two unrelated PIM2 shRNAs in CD34+ CML cells. Error bars indicate SD; n=3 technical replicates of a single experiment. (*B*) FACS analysis showing representative Annexin V/7-AAD staining of DMSO- or IM-treated human CMLSCs (CD34+CD38-CD90+) expressing a NS shRNA or one of two unrelated PIM2 shRNAs. These data provided the basis for the bar graph in Fig. 3*B*. (*C*) FACS analysis showing representative Annexin V/7-AAD staining of human CMLSCs (CD34+CD38-CD90+) treated with DMSO, IM, AZD1208 or both drugs. These data provided the basis for the bar graph in Fig. 3*D*. (*D*) Cell viability, as monitored by trypan blue cell counting, of CMLSCs (CD34+CD38-CD90+) cells treated with DMSO, IM, LGH447 or both drugs. Error bars indicate SEM; n=2 biological replicates. (*E*) Phospho-flow analysis showing intra-cellular staining of pBAD (S112) levels in CMLSCs (CD34+CD38-CD90+) treated with DMSO or LGH447. IgG was used for control staining. The upper panel shows a representative FACS histogram. The arithmetic mean fluorescence intensity (MFI) value is indicated in the boxed region. The upper panel shows the quantification of n=2 biological replicates. Error bars indicate SEM. (*F*) Cell viability of CMLSCs (CD34+CD38-CD90+) expressing a NS or STAT4 shRNA and treated in the presence or absence of IM. Error bars indicate SD; n=4 technical replicates of a single experiment. (*G*) Colony formation assay of human primary CD34+ CML cells treated with DMSO, IM, AZD1208 or both drugs. Error bars indicate SD; n=3 technical replicates. (*H*) Cell viability, as monitored by Presto blue cell proliferation assay, of KCL22 cells treated with DMSO, IM, AZD1208 or both drugs. Error bars indicate SEM; n=4 biological replicates. (*I*) Cell viability of K562R cells treated with DMSO, IM, AZD1208 or both drugs. Error bars indicate SEM; n=4 biological replicates. (*J*) Immunoblots monitoring levels of phosphorylated BAD (pBAD) and total BAD (tBAD) in K562 and K562R cells treated in the presence or absence of IM (left) or AZD1208 (right). β-actin (ACTB) was monitored as a loading control. The results show that treatment of IM-sensitive K562 cells with either IM or AZD1208 greatly reduced the levels of pBAD. By contrast, treatment of IM-resistant K562R cells with IM had a negligible effect on pBAD levels, whereas AZD1208 substantially reduced pBAD levels. (*K*) Cell viability of primary CML cells from IM-resistant patients harboring wild-type BCR-ABL (n=3) treated with DMSO, IM, AZD1208 or both drugs. Error bars indicate SEM. Matched samples from the same patient are indicated by dots of the same color. Statistical analysis was performed between the IM-treated group and combination treated group. Error bars indicate SEM. $*P \leq 0.05$, $**P \leq 0.01$.

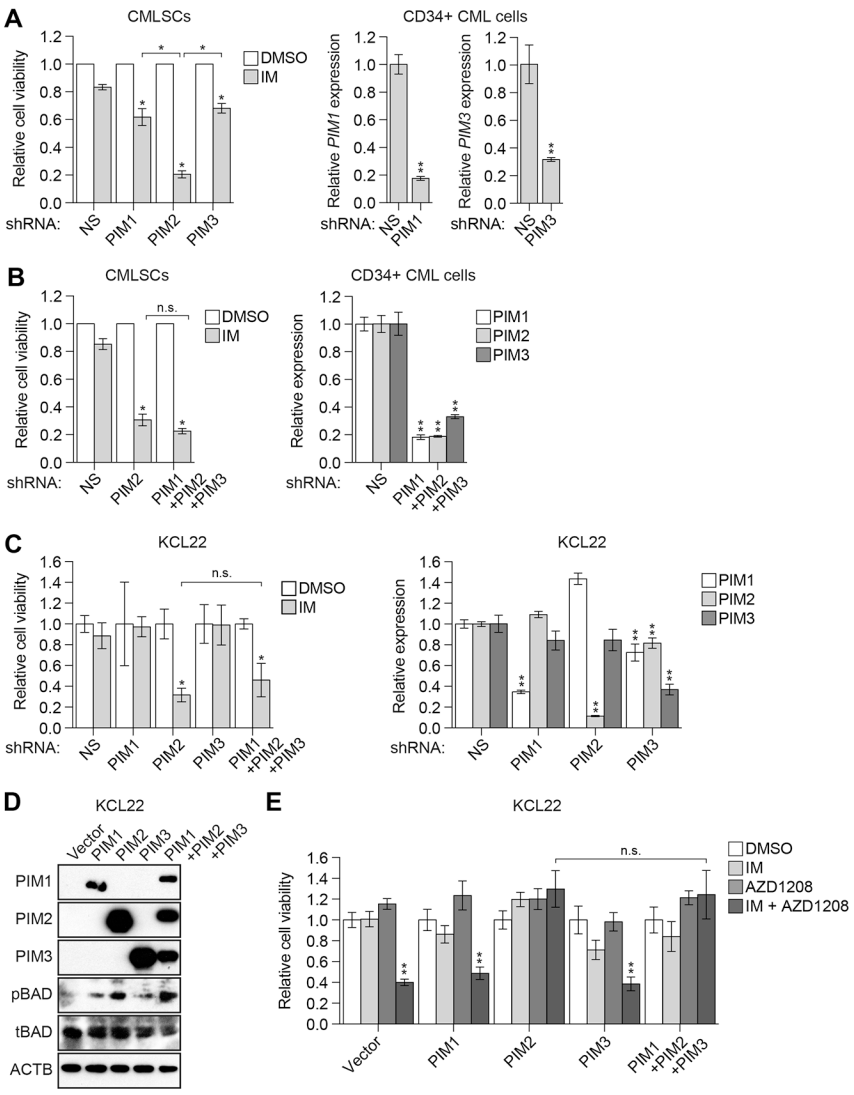

Fig. S10. Demonstration of PIM2 as the key mediator of IM resistance in IM-resistant CML cells. (*A*, *Left*) Relative cell viability of CMLSCs (CD34+CD38-CD90+) expressing a NS, PIM1, PIM2 or PIM3 shRNA and treated in the presence or absence of IM. Error bars indicate SEM; n=4 biological replicates. The results show that knockdown of PIM1 or PIM3 in CMLSCs resulted in only a minor sensitization to IM treatment (~1.5-fold reduction relative to a control non-silencing shRNA), whereas knockdown of PIM2 had a significantly greater effect (~5-fold). (*A*, *Center* and *right*) qRT-PCR monitoring knockdown efficiencies of PIM1 (Center) and PIM3 (Right) shRNAs in CD34+ CML cells. Error bars indicate SD; n=3 technical replicates of a single experiment. (*B*, *Left*) Relative cell viability of CMLSCs (CD34+CD38-CD90+) expressing a NS, PIM2, or PIM1, PIM2 and PIM3 shRNAs and treated in the presence or absence of IM. Error bars indicate SEM; n=4 biological replicates. The results show that knockdown of PIM1, PIM2 and PIM3 did not significantly affect IM sensitivity compared to knockdown of PIM2 alone. (*B*, *Right*) qRT-PCR monitoring *PIM* knockdown efficiencies of a construct expressing PIM1, PIM2 and PIM3 shRNAs in CD34+ CML cells. Error bars indicate SD; n=3 technical replicates of a single experiment. (*C*, *Left*) Relative cell viability of KCL22 cells expressing a NS, PIM1, PIM2 or PIM3 shRNA, or all three PIM shRNAs, and treated in the presence or absence of IM. Error bars indicate SD; n=4 technical replicates of a representative experiment (out of 2 experiments). (*C*,

Right) qRT-PCR monitoring knockdown efficiencies of PIM1, PIM2 and PIM3 in KCL22 cells. Error bars indicate SD; n=3 technical replicates of a single experiment. Asterisks indicate a significant decrease in expression (significant increases in expression are not indicated). The results confirm the specificity of each shRNA. (*D*) Immunoblot monitoring levels of pBAD in KLC22 cells expressing empty vector, or ectopically expressing PIM1, PIM2 and PIM3 either alone or in combination. The results show that overexpression of PIM2 increased the levels of pBAD, whereas overexpression of either PIM1 or PIM3 had a negligible effect on pBAD levels. Co-overexpression of PIM1, PIM2 and PIM3 did not increase pBAD levels compared to overexpression of PIM2 alone. (*E*) Relative cell viability of KCL22 cells expressing empty vector, or ectopically expressing PIM1, PIM2 and PIM3 either alone or in combination, and treated with IM, AZD1208 or both drugs. Error bars indicate SD; n=4 technical replicates of a representative experiment (out of at least 2 experiments). Asterisks indicate a significant decrease in cell viability (significant increases in cell viability are not indicated). The results show that overexpression of PIM2, but not PIM1 or PIM3, rescued the viability of KCL22 cells treated with IM and AZD1208. Notably, co-overexpression of PIM1, PIM2 and PIM3 did not enhance cell viability in the presence of AZD1208 compared to overexpression of PIM2 alone. Collectively, the results of A-E show that of the PIM family members, PIM2 (1) plays a key role in contributing to IM resistance of CMLSCs, (2) is the predominate regulator of pBAD levels, and (3) is the primary target of AZD1208. $*P \leq 0.05$, $**P \leq 0.01$, n.s denotes "not significant".

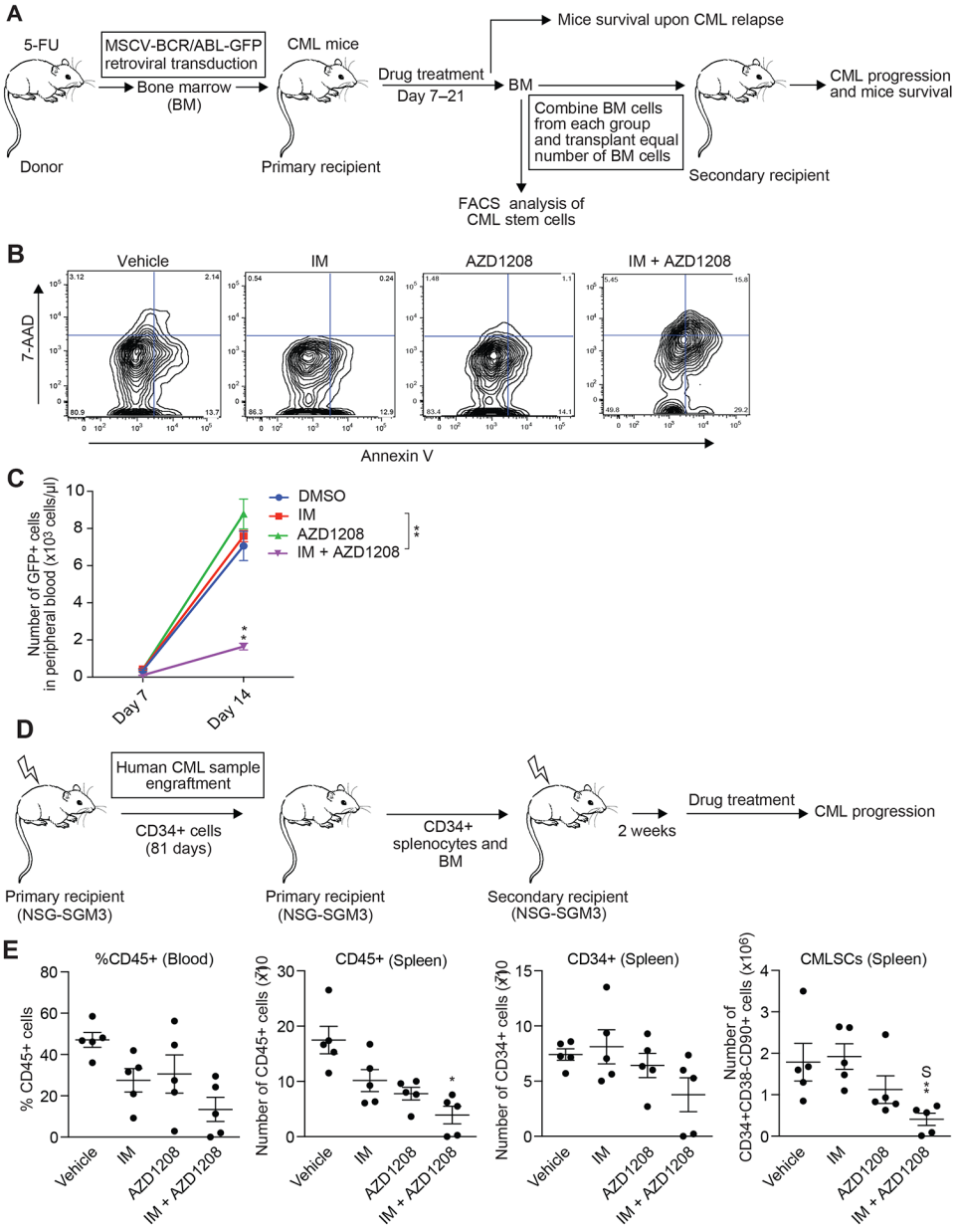

Fig. S11. Experimental schematic and additional supporting data for CML animal experiments. (*A*) Schematic of the CML mouse model experiments. CML was induced in mice using a retroviral transduction model. Seven days after bone marrow transplantation, CML mice were treated for two weeks with vehicle, IM, AZD1208, or both drugs. After drug discontinuation, some CML mice were sacrificed to harvest bone marrow cells to either analyze CMLSC apoptosis and viability or transplant into secondary recipients to monitor engraftment and animal survival. The remaining primary transplant CML mice were monitored for disease relapse and animal survival. (*B*) FACS analysis showing representative Annexin V/7-AAD staining of murine CML stem cells isolated from mice treated with vehicle, IM, AZD1208, or both drugs. These data provided the basis for the bar graph in Fig. 4*B*. (*C*) Expansion of CML (GFP+) cells in the peripheral blood of secondary recipient mice after receiving bone marrow cells from primary transplant mice treated with vehicle (n=5), IM (n=5), AZD1208 (n=5), or both drugs (n=5). Error bars indicate SEM. (*D*) Schematic of the PDX mouse experiment. (*E*) Percentage of CD45+ cells

in the peripheral blood, and number of CD45+ cells, CD34+ CML cells and CD34+CD38-CD90+ CMLSCs in the spleen of PDX mice (n=5 per group) engrafted with human CML cells and treated with vehicle, IM, AZD1208, or both drugs. S denotes the combined drug treatment was synergistic. Error bars indicate SEM. *$P \leq 0.05$, **$P \leq 0.01$.

Table S1. List of human CML patient samples used in this study

Sample ID	Source*	CML phase	BCR-ABL mutation status	Origin	Application (Figure)
CML1	UMass-CCTB	Newly-diagnosed chronic phase	Wild-type	Bone marrow	Fig. 1*A-C,* Fig. 2*A,* Fig. 3*A-E,* Fig. S1 (except Fig. S1*E*), Fig. S2-S4, Fig. S6*A*, Fig. S7*F* and *H*, Fig S9*A*, Fig. S11*E*
CML2	OHSU	Newly-diagnosed chronic phase	Wild-type	Bone marrow	Fig. 1*A-C*, Fig. 2*A*, Fig. 3*A-D*, Fig. S1 (except Fig. S1*E*), Fig. S2-S4
CML3	UMass-CCTB	Newly-diagnosed chronic phase	Wild-type	Bone marrow	Fig. 1*A-C*, Fig. 2*A*, *E* and *F*, Fig. 3*A-D*, Fig. S1 (except Fig. S1E), Fig. S2-S4, Fig. S6*B*, Fig. S9*D-F*, Fig. S10*A* and *B*
CML4	UMass-CCTB	Newly-diagnosed chronic phase	Wild-type	Bone marrow	Fig. S8*E* and *F*
CML5	UMass-CCTB	Newly-diagnosed chronic phase	Wild-type	Bone marrow	Fig. 3*E*
CML6	UMass-Path	Newly-diagnosed chronic phase	Wild-type	Bone marrow	Fig. 3*E*
CML7	UMass-Path	Newly-diagnosed chronic phase	Wild-type	Bone marrow	Fig. 3*E*
CML8	UMass-Path	IM resistant	Wild-type	Bone marrow	Fig. S9*K*
CML9	UMass-Path	IM resistant	Wild-type	Bone marrow	Fig. S9*K*
CML10	UMass-Path	IM resistant	Wild-type	Peripheral blood	Fig. S9*K*
CML11	UMass-CCTB	Newly-diagnosed chronic phase	Wild-type	Bone marrow	Fig. S1*E*
CML12	UMass-CCTB	Newly-diagnosed chronic phase	Wild-type	Bone marrow	Fig. S1*E*
CML13	UMass-CCTB	Newly-diagnosed chronic phase	Wild-type	Bone marrow	Fig. S1*E*

* OHSU, Druker Lab, OHSU Knight Cancer Institute; UMass-CCTB, UMass Cancer Center Tissue Bank; UMass-Path, Department of Pathology, University of Massachusetts Medical School.

Table S2. List of primer sequences used in this study.

Application	Gene	Forward primer (5'→3')	Reverse primer (5'→3')
Nested PCR	BCR-ABL (1st round)	GCAGCAGAAGAAGTGTTTCAG	CCGGAGCTTTTCACCTTTAG
	BCR-ABL (2nd round) (21)	CATTCCGCTGACCATCAATAA	AACGAGCGGCTTCACTCAGA
qRT-PCR	BCR-ABL (specific RT primer)	TGTTGACTGGCGTGATGTAGTTGCTTGG	
	B2M	GTATGCCTGCCGTGTGAAC	AAAGCAAGCAAGCAGAATTTGG
	GAPDH	TGCACCACCAACTGCTTAGC	GGCATGGACTGTGGTCATGAG
	PIM1	GGCTCGGTCTACTCAGGCA	GGAAATCCGGTCCTTCTCCAC
	PIM2 (human)	CTGACTTTGATGGGACAAGG	GAATCTCCTGGTCCCTCTC
	Pim2 (mouse)	ATCTCGCGACACCAGTACCAT	GATTAGGGCACAGCAATCTGG
	PIM3	AAGGACGAAAATCTGCTTGTGG	CGAAGTCGGTGTAGACCGTG
	STAT1	CAGCTTGACTCAAAATTCCTGGA	TGAAGATTACGCTTGCTTTTCCT
	STAT2	CCAGCTTTACTCGCACAGC	AGCCTTGGAATCATCACTCCC
	STAT3	CAGCAGCTTGACACACGGTA	AAACACCAAAGTGGCATGTGA
	STAT4	TGTTGGCCCAATGGATTGAAA	GGAAACACGACCTAACTGTTCAT
	STAT5A	GCAGAGTCCGTGACAGAGG	CCACAGGTAGGGACAGAGTCT
	STAT5B	GAGGTGCGGCATTATTTATCCC	GCGGTCATACGTGTTCTGGAG
	STAT6	GTTCCGCCACTTGCCAATG	TGGATCTCCCCTACTCGGTG
Cloning	PIM1 shRNA (into pLKO.1-GFP-PIM2 shRNA)	ACAGCAGAGATCCACTTTGGCCGCGGA CGAGACTAGCCTCGAGCG	CATACATCGATATACATAGCCAAAG TGGATCTCTGCTGTC
	PIM3 shRNA (into pLKO.1-GFP-PIM2 shRNA)	GCTATGTATATCGATGTATGACGAGAC TAGCCTCGAGCG	GCAACCCCAACCCCCTCGAGCCGCG GCAAAGTGGATCTCTGCTGTC
	PIM1 (into pHR-lentivirus)	TGGAGCTCTCGAGAATTCTCACGCGTG CCACCATGCTCTTGTCCAAAATCAACTC	GCGGATCCCATATGGGTACCACGCG TCTATTTGCTGGGCCCCGGCGACAG GCTG
	PIM2 (into pHR-lentivirus)	TGGAGCTCTCGAGAATTCTCACGCGTG CCACCATGTTGACCAAGCCTCTACAGG	GCGGATCCCATATGGGTACCACGCG TTAGGGTAGCAAGGACCAGGC
	PIM3 (into pHR-lentivirus)	TGGAGCTCTCGAGAATTCTCACGCGTG CCACCATGCTGCTCTCCAAGTTCGGCTC	GCGGATCCCATATGGGTACCACGCG TCACAAGCTCTCGCTGCTGGAC
	PIM1_2 P2A (into pHR_PGK)	CTGAAGCAGGCTGGAGACGTGGAGGA GAACCCTGGACCTATGTTGACCAAGCC TCTACAG	TCCACGTCTCCAGCCTGCTTCAGCA GGCTGAAGTTAGTAGCTCCGCTTCC TTTGCTGGGCCCCGGCGACAGGCTG
	PIM2_3 P2A (into pHR_PGK)	CTTCTAACATGCGGTGACGTGGAGGAG AATCCCGGCCCTATGCTGCTCTCCAAGT TCGGC	CCACGTCACCGCATGTTAGAAGACT TCCTCTGCCCTCACCAGAACCGGGT AGCAAGGACCAGGCCAAAG
	STAT5B shRNA (into pLKO.1-GFP-STAT5A shRNA)	ACAGCAGAGATCCACTTTGGCCGCGGA CGAGACTAGCCTCGAGCG	GCAACCCCAACCCCCTCGAGCCGCG GCAAAGTGGATCTCTGCTGTC
	STAT5A shRNA (into pLKO.1-GFP-STAT4 shRNA)	ACAGCAGAGATCCACTTTGGCCGCGGA CGAGACTAGCCTCGAGCG	CATACATCGATATACATAGCCAAAG TGGATCTCTGCTGTC
	STAT5B shRNA (into pLKO.1-GFP-STAT4 shRNA)	GCTATGTATATCGATGTATGACGAGAC TAGCCTCGAGCG	GCAACCCCAACCCCCTCGAGCCGCG GCAAAGTGGATCTCTGCTGTC
ChIP	PIM2 (TSS)	TGTACCACAGCCAATCGGAG	CACCTCAAGCCCCCTCATTT
	PIM2 (Exon 5)	GTGGATCTCTCGACACCAGT	TGTCATAGAGGAGGATGCCCA

Dataset S1. List of significantly differentially expressed genes (P < 0.01 and fold change > 1.5 or < 1/1.5) between CMLSCs and HSCs. A subgroup of the genes were used to generate the heatmaps and statistical analyses presented in Fig. 1A and Fig. S4.

References

1. Picelli S, *et al.* (2014) Full-length RNA-seq from single cells using Smart-seq2. *Nat Protoc* 9:171–181.
2. Trombetta JJ, *et al.* (2014) Preparation of Single-Cell RNA-Seq Libraries for Next Generation Sequencing. *Curr Protocol Mol Biol* 107:4.22.1–17.
3. Ihaka R, Gentleman R (1996) R: A language for data analysis and graphics. *J Compu. Graph Stat* 5:299–314.
4. Kim D, *et al.* (2013) TopHat2: accurate alignment of transcriptomes in the presence of insertions, deletions and gene fusions. *Genome Biol* 14:R36.
5. Anders S, Pyl PT, Huber W (2015) HTSeq--a Python framework to work with high-throughput sequencing data. *Bioinformatics* 31:166–169.
6. Li B, Dewey CN (2011) RSEM: accurate transcript quantification from RNA-Seq data with or without a reference genome. *BMC Bioinformatics* 12:323.
7. Hentschel J, *et al.* (2011) BCR-ABL- and Ras-independent activation of Raf as a novel mechanism of Imatinib resistance in CML. *Int J Oncol* 39:585–591.
8. Li WV, Li JJ (2018) An accurate and robust imputation method scImpute for single-cell RNA-seq data. *Nat Commun* 9:997.
9. Finak G, *et al.* (2015) MAST: a flexible statistical framework for assessing transcriptional changes and characterizing heterogeneity in single-cell RNA sequencing data. *Genome Biol* 16:278.
10. Law CW, Chen Y, Shi W, Smyth GK (2014) voom: Precision weights unlock linear model analysis tools for RNA-seq read counts. *Genome Biol* 15:R29.
11. Mi H, *et al.* (2010) PANTHER version 7: improved phylogenetic trees, orthologs and collaboration with the Gene Ontology Consortium. *Nucleic Acids Res* 38:D204–210.
12. Zhang B, *et al.* (2016) Heterogeneity of leukemia-initiating capacity of chronic myelogenous leukemia stem cells. *J Clin Invest* 126:975–991.
13. Ma L, *et al.* (2014) A therapeutically targetable mechanism of BCR-ABL-independent imatinib resistance in chronic myeloid leukemia. *Sci Transl Med* 6:252ra121.
14. Gerber JM, *et al.* (2013) Genome-wide comparison of the transcriptomes of highly enriched normal and chronic myeloid leukemia stem and progenitor cell populations. *Oncotarget* 4:715–728.
15. Zhang B, *et al.* (2013) Microenvironmental protection of CML stem and progenitor cells from tyrosine kinase inhibitors through N-cadherin and Wnt-beta-catenin signaling. *Blood* 121:1824–1838.
16. Zhang B, *et al.* (2010) Effective targeting of quiescent chronic myelogenous leukemia stem cells by histone deacetylase inhibitors in combination with imatinib mesylate. *Cancer Cell* 17:427–442.
17. Ritchie ME, *et al.* (2015) limma powers differential expression analyses for RNA-sequencing and microarray studies. *Nucleic Acids Res* 43:e47.
18. Gazin C, Wajapeyee N, Gobeil S, Virbasius CM, Green MR (2007) An elaborate pathway required for Ras-mediated epigenetic silencing. *Nature* 449:1073–1077.
19. Chen Y, Hu Y, Zhang H, Peng C, Li S (2009) Loss of the Alox5 gene impairs leukemia stem cells and prevents chronic myeloid leukemia. *Nat Genet* 41:783-792.
20. Nelson EA, *et al.* (2011) The STAT5 inhibitor pimozide decreases survival of chronic myelogenous leukemia cells resistant to kinase inhibitors. *Blood* 117:3421–3429.

21. Chu S, Holtz M, Gupta M, Bhatia R (2004) BCR/ABL kinase inhibition by imatinib mesylate enhances MAP kinase activity in chronic myelogenous leukemia CD34+ cells. *Blood* 103:3167–3174.